Oct 19th, 12:00 AM

A Design Approach for Complex Stiffeners

Andrew T. Sarawit

Teoman Pekoz

Fifteenth International Specialty Conference on Cold-Formed Steel Structures
St. Louis, Missouri U.S.A., October 19-20, 2000

A Design Approach for Complex Stiffeners

A. T. Sarawit[1], T. Peköz[2]

ABSTRACT

This paper presents a design approach for laterally braced cold-formed steel flexural members with edge stiffened flanges other then simple lips. The design method for flexural members given by Schafer and Peköz (1999) is used here for designing these complex stiffeners. The method integrates distortional buckling into the unified effective width approach currently used in most cold-formed steel design specifications. A finite element method was first used to investigate the post-buckling behavior and carry out initial geometric imperfection sensitivity studies for various types of stiffeners. Then parametric studies were carried out for different types of stiffeners to compare the moment capacity determined by the finite element method, AISI (1996) and the proposed design approach for flexural members given by Schafer and Peköz (1999).

INTRODUCTION

The following is a summary of the design procedures for flexural members given by Schafer and Peköz (1999). The design procedures are based on the need for the integration of the distortional mode into the design procedure. Two behavioral phenomena must be considered. First, the distortional mode has less post-buckling capacity than the local mode. Second, the distortional mode has the ability to control failure even when it occurs at a higher critical stress than the local mode. A design method incorporating these phenomena is needed to provide an integrated approach to strength prediction involving local and distortional buckling. For consistency with the existing cold-form steel design specifications an effective width approach was undertaken. Effective section properties are based on effective widths, *b*.

[1] Graduate Research Assistant, School of Civil and Environmental Engineering, Cornell University, Ithaca, NY 14850, U.S.A.

[2] Professor, School of Civil and Environmental Engineering, Cornell University, Ithaca, NY 14850, U.S.A.

$$b = \rho w \tag{1}$$

where w is the actual element width and post-buckling reduction factor, ρ, is

$$\rho = (1 - 0.22/\lambda)/\lambda \text{ for } \lambda > 0.673 \text{ otherwise } \rho = 1. \tag{2}$$

where

$$\lambda = \sqrt{f_y / f_{cr}} \tag{3}$$

In order to properly integrate distortional buckling, reduced post-buckling capacity in the distortional mode and the ability of the distortional mode to control the failure mechanism even when at a higher buckling stress than the local mode must be incorporated. Therefore, the critical buckling stress of the element was defined by comparing the local buckling stress and distortional buckling stress to determine the governing mode as follows:

$$(f_{cr}) = \min\left[(f_{cr})_{local}, R_d (f_{cr})_{dist.}\right] \tag{4}$$

$$R_d = \min\left(1, \frac{1.17}{\lambda_d + 1} + 0.3\right) \text{ where } \lambda_d = \sqrt{f_y / (f_{cr})_{dist.}} \tag{5}$$

R_d reflects the reduced strength in mechanisms associated with distortional failures. For $R_d < 1$ this method provides an additional reduction on the post-buckling capacity. Further, the method allows the distortional mode to control situations where the distortional buckling stress is greater than the local buckling stress. Thus, R_d provides a framework for solving the problem of predicting the failure mode and reducing the post-buckling capacity in the distortional mode. Schafer and Peköz (1999) developed the expression for R_d based on post-buckling capacity as shown in Figure 3 (a) and from the experimental results of Hancock et al. (1994). With f_{cr} of the element known the effective width of each element may readily be determined and the effective section properties generated.

IMPERFECTION SENSITIVITY STUDY

To investigate the post-buckling behavior and develop the expression for R_d the authors analyzed an isolated flange-stiffener model as shown in Figure 3 (a) rather then using the full section. Two types of imperfections, local and distortional mode, are superposed to give the initial geometric imperfections. The magnitude of the imperfection is selected based on the statistical summary provided in Schafer and Peköz (1998). Then the ultimate strength of these isolated flanges is found for different magnitudes of imperfection. Two maximum imperfection

magnitudes, one at 25% and the other at 75% probability of exceedance, are used. The percent differences in the strength are used to measure the imperfection sensitivity.

$$\frac{(f_u)_{75\%imp.} - (f_u)_{25\%imp.}}{\frac{1}{2}\left((f_u)_{75\%imp.} + (f_u)_{25\%imp.}\right)} \times 100\% \quad (6)$$

The error bars in Figure 3 (a) show the range of strengths predicted for imperfections varying over the central 50% portion of expected imperfection magnitudes. The greater the error bars, the greater the imperfection sensitivity. A contour plot of this imperfection sensitivity statistic is shown in Figure 3 (b). Stocky members tending to failure in the distortional mode have the highest sensitivity.

The design approach given by Schafer and Peköz (1999) was developed based on simple lips edge stiffeners. Therefore, before adopting this approach for other types of stiffeners verification on the reduction factor for distortional stress, R_d is needed. This is done by creating a post-buckling capacity graph and imperfection sensitivity contour plot on the types of stiffeners in interest for comparison with the original Figure 3 (a) and 3 (b). In this research 4 types of complex stiffeners shown in Figure 4 (a), 5 (a), 6 (a) and 7 (a) are studied.

Finite Element Model

In order to study the post-buckling behavior of complex stiffened elements nonlinear finite element analyses are performed using ABAQUS. To study only the complex stiffened element behavior an idealization of the boundary conditions at the web/flange junction are made by restraining all degrees of freedom except for the translation along the length. Roller supports are used at both ends and to avoid localized failure at the ends the uniform load has been distributed to the first row of elements. Boundary conditions are shown in Figure 2. The material model used is elastic-plastic with strain hardening and fy = 347 MPa. Residual stress is also included with a 30% yield stress throughout the thickness in the longitudinal direction. The residual stresses are assumed tension on the outside and compression on the inside of the section.

Initial geometric imperfection is introduced by superimposing the eigenmodes for the local and distortional buckling shown in Figure 1. The magnitude of the imperfection is selected based on the statistical summary provided in Schafer and Peköz (1998). The length of the model is selected by using the length that would give the least buckling strength in the distortional mode, which is obtained, by using the Finite Strip Method CUFSM. Table 1 summarizes the

geometry of the members. An investigation of the post-buckling behavior and an imperfection sensitivity study has been performed for each type of stiffener. Figures 4, 5, 6 and 7 show the results. For each type of stiffener a total of 42 models were investigated.

It can be seen that the post-buckling capacity graphs and imperfection sensitivity contour plots are similar to those obtained by simple lips edge stiffened flanges. Therefore, the reduction factor for distortional stress, R_d is expected to be similar to Schafer and Peköz (1999).

PARAMETRIC STUDIES

Two Z-section parametric studies were carried out for different types of stiffeners to compare the moment capacity as determined by the finite element method, AISI (1996) and the proposed design approach for flexural members given by Schafer and Peköz (1999). The first parameter study consists of different Z-section geometry with all cross sections having the same thickness while the second parametric study uses one standard Z-section with variation in thickness. The cross sections selected for both these parameter studies are intend to cover a wide range of slenderness.

Parametric Study I

The parametric study was carried out by changing different widths of the web, flanges and stiffeners for five types of stiffeners simple lips, inside angled, outside angled, inside hooked, and outside hooked stiffeners. All cross sections have the same thickness. Figure 8 (b)-(f) and Table 2 summarize the geometry of the members. Local and distortional buckling stresses obtained by the finite strip method are used for the proposed design approach for flexural members given by Schafer and Peköz (1999).

Finite Element Model

The finite element model used for this parametric study is shown in Figure 9 (a). The web/flange junction is restrained only for the translation degree of freedom perpendicular to the length to brace the member laterally. Roller supports are used at both ends. To avoid localized failure at the ends the constant moment is modeled by nodal loads distributed to the first row of elements. The material model used is elastic-plastic with strain hardening and fy = 345 MPa. Residual stress throughout the thickness in the longitudinal direction is assumed to be 30% of the

yield stress in the flange and 40% of the yield stress in the web. The residual stresses are also assumed to be tension on the outside and compression on the inside of the section.

Initial geometric imperfections are introduced by superimposing the eigenmodes for the local and distortional buckling shown in Figure 9 (b) and (c). Two different imperfection magnitudes of 75% and 25% probability of exceedance, based on the statistical summary provided in Schafer and Peköz (1998), are used for each model. The length of the model is selected by using three half-wave lengths of the distortional mode that gives the least buckling strength. The wavelengths are obtained using the Finite Strip Method. Figures 10 (a), 11 (a) and 12 (a) summarize the results for the different approaches.

Parametric Study II

The second parametric study was carried out by modifying the stiffeners of a standard cross section 12ZS3.25, which has a depth of 12 inches, flange width of 3.25 inches and with a sloping edge stiffener. The sloping stiffener was modified into simple lips, inside angled and outside angled stiffeners. Figure 8 (a)–(d) summarize the geometry of the members. This was done for different thicknesses: 0.135, 0.105, 0.090, 0.075 and 0.060 inches. The finite element assumptions are the same as in the first parameter study except for the yield stress and the lateral bracing conditions. This study uses a 55 ksi yield stress and instead of fully bracing along the length as in the first parameter study, only four brace points are used. Brace points included one at each end and additional ones at one-third of the length, which is the same length as the half-wave lengths of the distortional mode which gives the least buckling strength. For these cross sections and bracing lengths, full formation of the distortional mode is still possible without causing a lateral-torsional failure. Figures 10 (b), 11 (b) and 12 (b) summarize the results for the different approaches.

SUMMARY AND CONCLUSIONS

Results from the investigation of the post-buckling behavior and imperfection sensitivity studies on different types of stiffeners suggest that the reduction factor for distortional stress, R_d given by to Schafer and Peköz (1999) may still be used for stiffeners other then simple lips.

Results from the first and second parametric studies revealed that the AISI (1996) approach gives unconservative moment capacity while the proposed design approach for flexural

members given by Schafer and Peköz (1999) gives a more conservative result closer to the finite element results. There are no physical test results for these kinds of complex stiffeners. Tests for members with cross sections such as in Figure 8 are needed to verify this approach. Furthermore, study of section optimization with complex stiffeners should be conducted.

ACKNOWLEDGEMENT

The sponsorship of the American Iron and Steel Institute and the help of D.L Johnson, Chair of the AISI Subcommittee in charge of this project, Dr. Helen Chen of the AISI and Dr. B. W. Schafer are gratefully acknowledged.

REFERENCES

American Iron and Steel Institute, (1996). AISI Specification for the Design of Cold-Formed Steel Structural Members. *American Iron and Steel Institute* Washington, D.C.

Peköz, T., (1987). *Development of a Unified Approach to the Design of Cold-Formed Steel Members*. American Iron and Steel Institute Research Report CF 87-1.

Schafer, B.W., (1997). "Cold-Formed Steel Behavior and Design: Analytical and Numerical Modeling of Elements and Members with Longitudinal Stiffeners." Ph.D. Dissertation, Cornell University, Ithaca, New York

Schafer, B.W., and Peköz, T.P., (1999). "Laterally Braced Cold-Formed Steel Flexural Members with Edge Stiffened Flanges." *Journal of Structural Engineering,* 125(2)

Schafer, B.W., "CUFSM, Cornell University Finite Strip Method User's Manual v1.0d" Cornell University, Ithaca, New York

Table 1 Summary of Isolated Flange-Stiffener Models Geometry*

B	D	a
25	6.25	0, 3.125, 6.25
	12.5	0, 6.25, 12.5
50	6.25	0, 3.125, 6.25
	12.5	0, 6.25, 12.5
	25	0, 12.5, 25
75	6.25	0, 3.125, 6.25
	12.5	0, 6.25, 12.5
	25	0, 12.5, 25
	37.5	0, 18.75, 37.5
100	6.25	0, 3.125, 6.25
	12.5	0, 6.25, 12.5
	25	0, 12.5, 25
	37.5	0, 18.75, 37.5
	50	0, 25, 50

*Thickness = 1 mm in all cases

Table 2 Summary of Z-section Models Geometry*

Model	H	B	d	a
1	50	25	6.25	3.125
2	50	25	6.25	6.25
3	100	25	6.25	3.125
4	100	25	6.25	6.25
5	100	50	6.25	3.125
6	100	50	6.25	6.25
7	100	50	12.5	6.25
8	100	50	12.5	12.5
9	150	25	6.25	3.125
10	150	25	6.25	6.25
11	150	50	6.25	3.125
12	150	50	6.25	6.25
13	150	50	12.5	6.25
14	150	50	12.5	12.5

* Thickness = 1 mm in all cases

Table 3 Summary of Z-section Moment Capacity for Parametric Study I

Model	Simple lips				Inside Angled				Outside Angled				Inside Hooked				Outside Hooked			
	$M_{75\%}$ (N-m)	$M_{25\%}$ (N-m)	$\frac{M_{AISI}}{M_{50\%}}$	$\frac{M_{PRO}}{M_{50\%}}$	$M_{75\%}$ (N-m)	$M_{25\%}$ (N-m)	$\frac{M_{AISI}}{M_{50\%}}$	$\frac{M_{PRO}}{M_{50\%}}$	$M_{75\%}$ (N-m)	$M_{25\%}$ (N-m)	$\frac{M_{AISI}}{M_{50\%}}$	$\frac{M_{PRO}}{M_{50\%}}$	$M_{75\%}$ (N-m)	$M_{25\%}$ (N-m)	$\frac{M_{AISI}}{M_{50\%}}$	$\frac{M_{PRO}}{M_{50\%}}$	$M_{75\%}$ (N-m)	$M_{25\%}$ (N-m)	$\frac{M_{AISI}}{M_{50\%}}$	$\frac{M_{PRO}}{M_{50\%}}$
1	718	613	1.027	1.027	709	596	1.055	1.055	702	594	1.062	1.057	710	596	1.056	1.056	710	637	1.024	1.014
2	757	691	0.960	0.968	755	635	1.034	1.034	740	654	1.031	0.987	746	630	1.053	1.053	724	617	1.080	1.033
3	1665	1551	1.060	0.987	1647	1517	1.081	0.989	1708	1532	1.055	0.931	1616	1503	1.098	0.995	1643	1523	1.081	0.952
4	1823	1650	1.008	0.956	1753	1558	1.083	1.012	1764	1583	1.071	0.907	1744	1584	1.080	0.988	1674	1536	1.120	0.951
5	1684	1650	1.177	1.052	1556	1536	1.324	1.092	1922	1708	1.128	0.906	1513	1480	1.361	1.114	1498	1488	1.365	1.095
6	2174	1845	1.097	0.991	1832	1569	1.265	1.067	2015	1784	1.132	0.886	1703	1602	1.296	1.067	1722	1668	1.263	0.980
7	2292	1994	1.032	1.036	2360	2002	1.098	1.042	2371	2008	1.094	0.984	2362	2058	1.086	1.014	2364	2003	1.099	0.983
8	2430	2243	0.916	0.961	2470	2059	1.110	1.064	2435	2056	1.120	0.942	2453	2114	1.111	1.047	2433	2080	1.125	0.945
9	2719	2544	1.101	0.872	2595	2404	1.162	0.917	2604	2486	1.141	0.883	2623	2442	1.147	0.911	2644	2487	1.132	0.877
10	2916	2794	1.040	0.835	2850	2693	1.097	0.863	2702	2544	1.159	0.874	2869	2726	1.089	0.870	2736	2581	1.146	0.868
11	2766	2719	1.105	1.005	2709	2688	1.187	0.982	3115	2947	1.057	0.853	2387	2369	1.340	1.105	2430	2361	1.330	1.079
12	3160	2815	1.168	1.037	2666	2452	1.323	1.106	2448	2216	1.452	1.132	2522	2371	1.375	1.123	2308	2251	1.476	1.148
13	3736	3356	0.983	0.948	3856	3521	1.048	0.920	3777	3567	1.053	0.908	3949	3586	1.028	0.901	3939	3539	1.035	0.891
14	3766	3508	0.919	0.958	4130	3696	1.042	0.912	3964	3588	1.080	0.871	4178	3708	1.045	0.911	4041	3547	1.086	0.874
		Avg.	1.042	0.974		Avg.	1.136	1.004		Avg.	1.117	0.937		Avg.	1.155	1.011		Avg.	1.169	0.978

$M_{75\%}$, $M_{25\%}$ – Ultimate moment capacity by finite element method for imperfection magnitudes 75% and 25% probability of exceedance
$M_{50\%} = (M_{25\%} + M_{75\%})/2$
M_{AISI}, M_{PRO} - Nominal Moment capacity by AISI and proposed design approach for flexural members given by Schafer and Peköz (1999)

Table 4 Summary of Z-section Moment Capacity for Parametric Study II

Thickness	Simple lips				Simple lips				Inside Angled				Outside Angled			
	$M_{75\%}$ (kip-in.)	$M_{25\%}$ (kip-in.)	$\frac{M_{AISI}}{M_{50\%}}$	$\frac{M_{PRO}}{M_{50\%}}$	$M_{75\%}$ (kip-in.)	$M_{25\%}$ (kip-in.)	$\frac{M_{AISI}}{M_{50\%}}$	$\frac{M_{PRO}}{M_{50\%}}$	$M_{75\%}$ (kip-in.)	$M_{25\%}$ (kip-in.)	$\frac{M_{AISI}}{M_{50\%}}$	$\frac{M_{PRO}}{M_{50\%}}$	$M_{75\%}$ (kip-in.)	$M_{25\%}$ (kip-in.)	$\frac{M_{AISI}}{M_{50\%}}$	$\frac{M_{PRO}}{M_{50\%}}$
0.135	436	378	1.150	0.985	433	411	1.133	1.020	420	368	1.231	1.039	420	376	1.219	0.995
0.105	262	267	1.247	1.049	283	264	1.250	1.111	269	270	1.288	1.054	257	264	1.336	1.048
0.090	194	185	1.397	1.163	221	214	1.276	1.121	213	207	1.375	1.170	192	188	1.518	1.139
0.075	141	135	1.404	1.218	170	174	1.192	1.088	149	145	1.425	1.173	141	135	1.523	1.191
0.060	94	91	1.452	1.295	122	118	1.213	1.129	112	100	1.366	1.165	97	95	1.505	1.213
		Avg.	1.330	1.142		Avg.	1.213	1.094		Avg.	1.337	1.120		Avg.	1.420	1.117

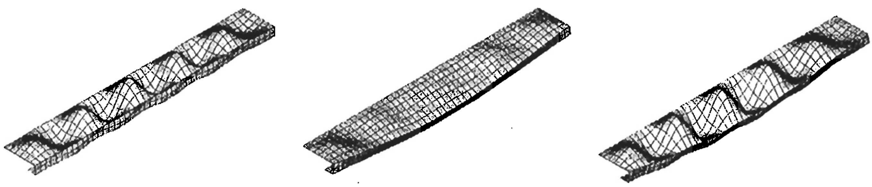

Figure 1 Isolated Flange-Stiffener (a) Local Buckling (b) Distortional Buckling (c) Geometric Imperfection

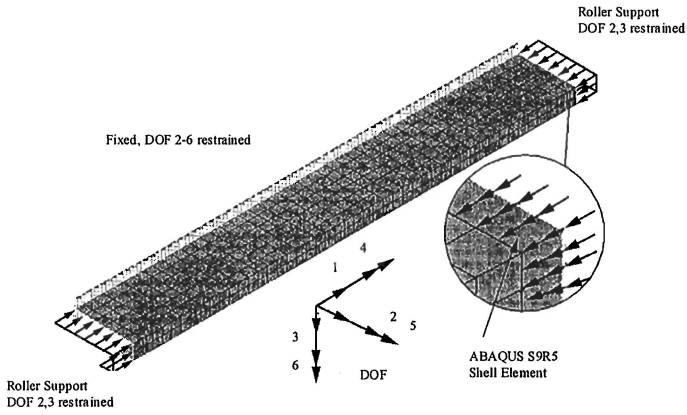

Figure 2 Isolated Flange-Stiffener Boundary Conditions

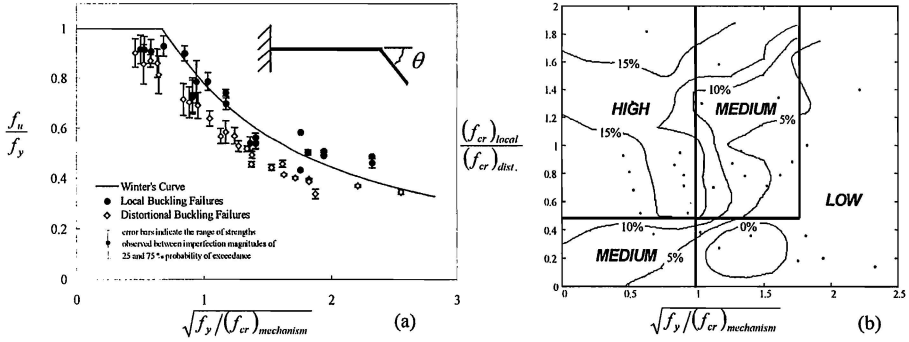

Figure 3 Simple Lips Stiffener (a) Post-Buckling Capacity (b) Imperfection Sensitivity

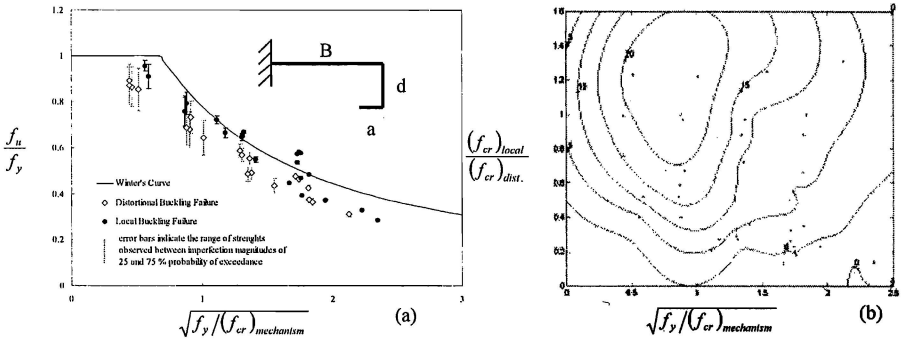

Figure 4 Inside Angled Stiffener (a) Post-Buckling Capacity (b) Imperfection Sensitivity

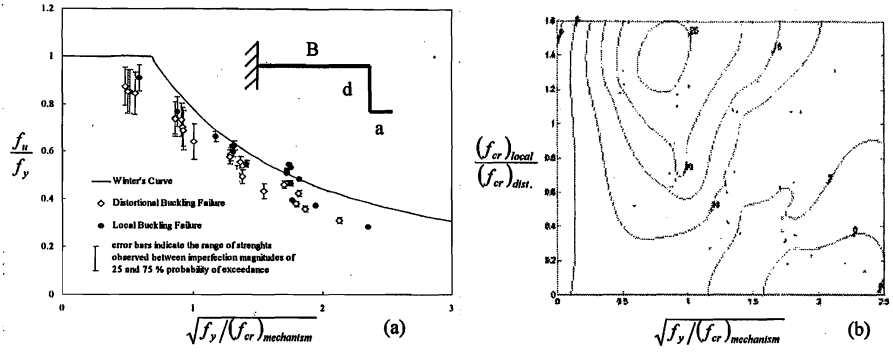

Figure 5 Outside Angled Stiffener (a) Post-Buckling Capacity (b) Imperfection Sensitivity

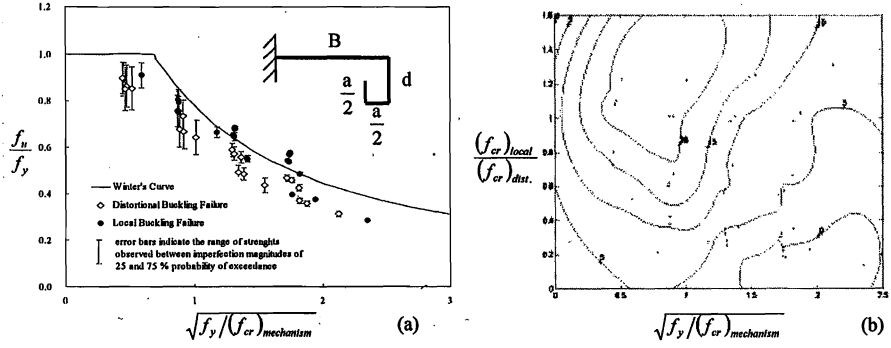

Figure 6 Inside Hooked Stiffener (a) Post-Buckling Capacity (b) Imperfection Sensitivity

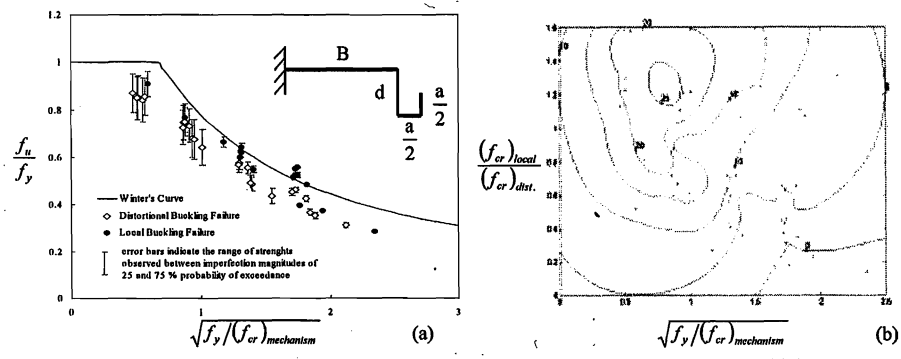

Figure 7 Outside Hooked Stiffener (a) Post-Buckling Capacity (b) Imperfection Sensitivity

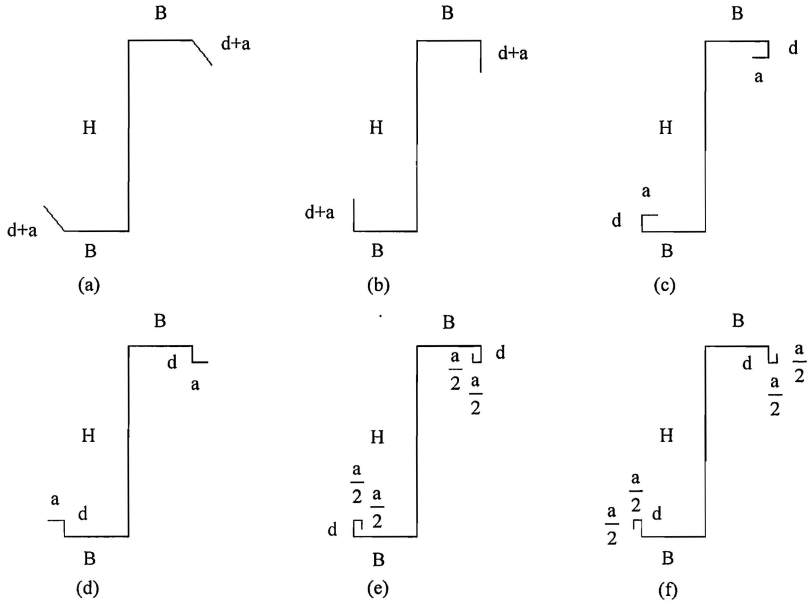

Figure 8 Z-section with (a) Sloping Lips Stiffener 50-degree respect to the flange (b) Simple Lips Stiffener (c) Inside Angled Stiffener (d) Outside Angled Stiffener (e) Inside Hooked Stiffener (f) Outside Hooked Stiffener

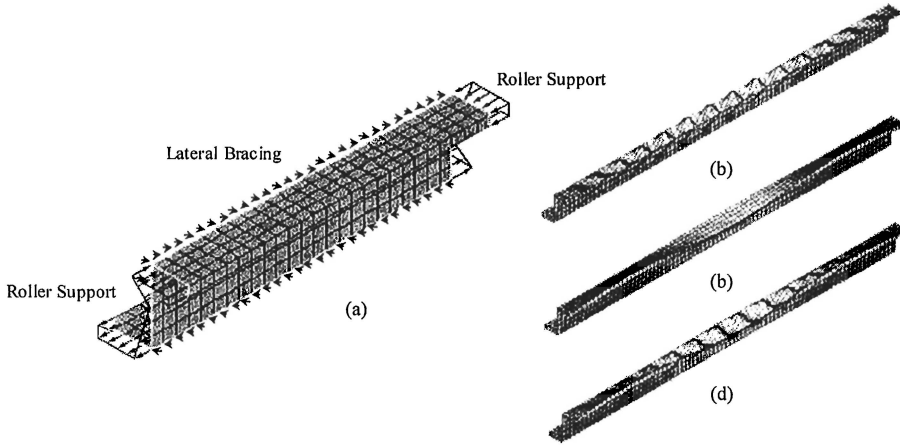

Figure 9 (a) Boundary Conditions (b) Local Buckling (c) Distortional Buckling (d) Initial Geometric Imperfection

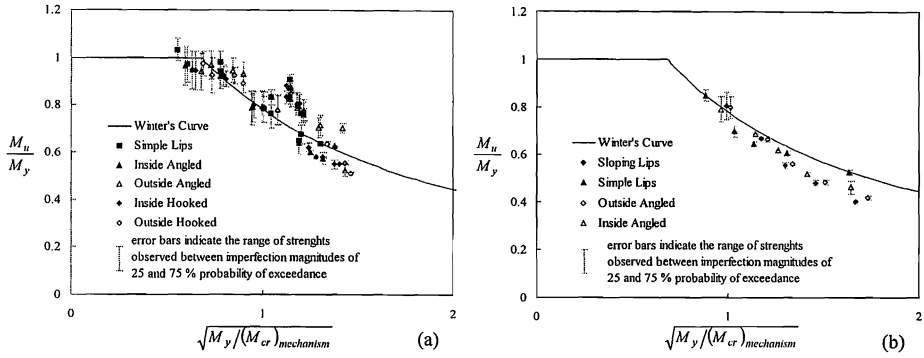

Figure 10 Post-Buckling Capacity by Finite Element Method (a) Parametric Study I (b) Parametric Study II

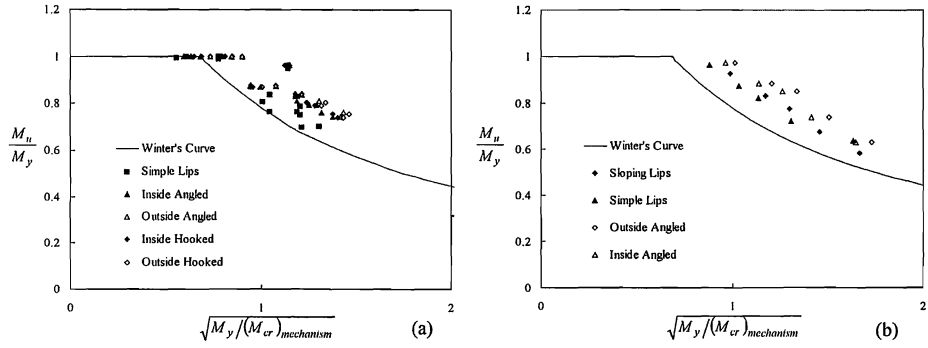

Figure 11 Post-Buckling Capacity by AISI Method (a) Parametric Study I (b) Parametric Study II

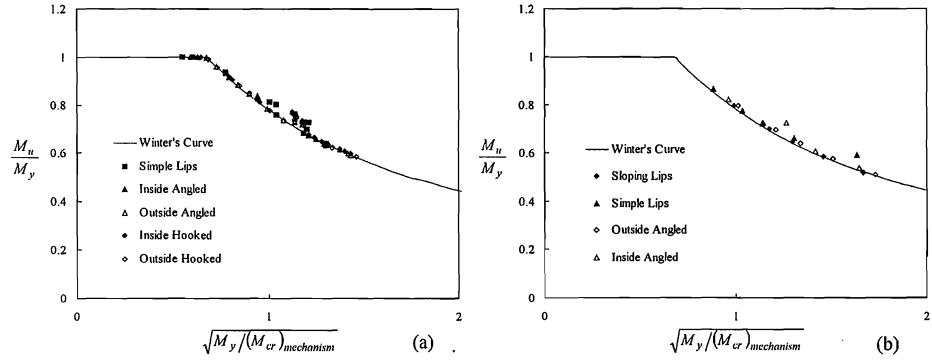

Figure 12 Post-Buckling Capacity by Propose Method (a) Parametric Study I (b) Parametric Study II